Receptor-type guanylate cyclase is required for carbon dioxide sensation by *Caenorhabditis elegans*

Elissa A. Hallem[a,1], W. Clay Spencer[b], Rebecca D. McWhirter[b], Georg Zeller[c,d,2], Stefan R. Henz[d], Gunnar Rätsch[c], David M. Miller III[b], H. Robert Horvitz[e], Paul W. Sternberg[a,3], and Niels Ringstad[e,f,3]

[a]Howard Hughes Medical Institute, Division of Biology, California Institute of Technology, Pasadena, CA 91125; [b]Department of Cell and Developmental Biology, Vanderbilt University School of Medicine, Nashville, TN 37232; [c]Friedrich Miescher Laboratory of the Max Planck Society, 72076 Tübingen, Germany; [d]Department of Molecular Biology, Max Planck Institute for Developmental Biology, 72076 Tübingen, Germany; [e]Howard Hughes Medical Institute, Department of Biology and McGovern Institute for Brain Research, Massachusetts Institute of Technology, Cambridge, MA 02139; and [f]Department of Cell Biology and the Helen L. and Martin S. Kimmel Center for Biology and Medicine at the Skirball Institute of Biomolecular Medicine, New York University Langone Medical Center, New York NY 10016

Contributed by Paul W. Sternberg, November 22, 2010 (sent for review August 2, 2010)

CO_2 is both a critical regulator of animal physiology and an important sensory cue for many animals for host detection, food location, and mate finding. The free-living soil nematode *Caenorhabditis elegans* shows CO_2 avoidance behavior, which requires a pair of ciliated sensory neurons, the BAG neurons. Using in vivo calcium imaging, we show that CO_2 specifically activates the BAG neurons and that the CO_2-sensing function of BAG neurons requires TAX-2/TAX-4 cyclic nucleotide-gated ion channels and the receptor-type guanylate cyclase GCY-9. Our results delineate a molecular pathway for CO_2 sensing and suggest that activation of a receptor-type guanylate cyclase is an evolutionarily conserved mechanism by which animals detect environmental CO_2.

guanylyl cyclase | olfaction | transcriptional profiling | regulator of G protein signaling | chemosensation

The ability to detect and respond to changing concentrations of environmental CO_2 is widespread among animals and plays a critical role in locating food, finding hosts and mates, and avoiding danger (1–4). CO_2 exposure can also have profound physiological effects, including altered respiration, motility, fecundity, and emotional state (5–7). CO_2 is sensed as an aversive cue by many free-living animals, including humans (3, 6, 8, 9). By contrast, many parasites and disease vectors are attracted to CO_2, which serves as a sensory cue for host location (1, 10).

Nematodes constitute a large and highly diverse phylum that includes both free-living and parasitic species. Many parasitic nematodes, including some of the most devastating human- and plant-parasitic nematodes, are attracted to CO_2. By contrast, adults of the free-living species *Caenorhabditis elegans* are repelled by CO_2 (11–14). CO_2 avoidance by *C. elegans* requires a pair of head neurons called the BAG neurons (13), which also mediate responses to decreases in ambient oxygen levels (15). Whether the BAG neurons directly sense CO_2 is not known, and the signaling pathways that mediate CO_2 detection are poorly understood.

We show here that environmental CO_2 specifically activates the BAG neurons and not other neurons that drive avoidance behavior, suggesting that the BAG neurons are primary sensory neurons that detect CO_2. Prolonged CO_2 exposure causes desensitization of avoidance behavior and the BAG neurons themselves, indicating that behavioral adaptation to CO_2 occurs at the level of the BAG neurons. In addition, we show that the CO_2-evoked activity of the BAG neurons requires a cGMP signaling pathway consisting of the receptor guanylate cyclase GCY-9 and the cGMP-gated cation channel TAX-2/TAX-4. Insects detect CO_2 using a pair of gustatory receptors (16, 17), whereas some mammals detect CO_2 using the receptor-type guanylate cyclase, guanylate cyclase D (GC-D), and soluble adenylate cyclase (18–20). Our results show that the mechanism of CO_2 detection in *C. elegans* more closely resembles that of mammals than insects and suggest an evolutionarily ancient role for receptor-type guanylate cyclases in mediating environmental CO_2 detection by animals.

Results

BAG Neurons Are Activated by CO_2. BAG neurons are located in the head, extend ciliated dendrites to the tip of the nose (21), and are required for avoidance of CO_2 across concentrations (Figs. S1 and S2). To determine whether the BAG neurons respond to environmental CO_2, we monitored the activity of BAG neurons using the genetically encoded ratiometric calcium indicator cameleon (22). The *gcy-33* promoter was used to drive expression of cameleon specifically in the BAG neurons (23). We first confirmed that animals expressing *gcy-33::cameleon* show normal CO_2 avoidance behavior (Fig. S3). We then imaged these animals and found that CO_2 exposure evoked rapid and reversible calcium transients in the cell bodies of BAG neurons (Fig. 1*A* and Fig. S4). By contrast, other sensory neurons known to mediate *C. elegans* avoidance behavior, the amphid neurons ASH, ADL, and AWB, did not respond to a 10% CO_2 stimulus, indicating that the CO_2 response of BAG neurons is cell type-specific (Fig. 1*B*). This result suggests that the BAG neurons are the primary sensory neurons that detect CO_2.

Prolonged CO_2 Exposure Desensitizes BAG Neurons. Prolonged exposure to many sensory stimuli results in behavioral adaptation, which can occur either in the primary sensory neuron or in circuitry downstream of the sensory neuron (24–28). We tested whether CO_2 avoidance behavior adapts to prolonged CO_2 exposure by exposing animals to 1%, 5%, or 10% CO_2 for either 1 or 5 min and then testing their ability to respond to 5% or 10% CO_2 in an acute avoidance assay. We found that prolonged exposure to either 5% or 10% CO_2 greatly reduced subsequent behavioral responses to the same concentration of CO_2, and responses to 10% CO_2 were significantly decreased after a 1-min

Author contributions: E.A.H., D.M.M., H.R.H., P.W.S., and N.R. designed research; E.A.H., N.R., W.C.S., and R.D.M. performed research; E.A.H., G.Z., S.R.H., G.R., and N.R. analyzed data; and E.A.H., H.R.H., P.W.S., and N.R. wrote the paper.

The authors declare no conflict of interest.

Freely available online through the PNAS open access option.

Data deposition: The sequence reported in this paper has been deposited in the GenBank database (accession no. HQ636455). The gene expression data have been deposited in the Gene Expression Omnibus database (accession no. GSE23769).

[1]Present address: Department of Microbiology, Immunology, and Molecular Genetics, University of California, Los Angeles, CA 90095.

[2]Present address: Structural and Computational Biology Unit, European Molecular Biology Laboratory, 69117 Heidelberg, Germany.

[3]To whom correspondence may be addressed. E-mail: pws@caltech.edu or niels.ringstad@med.nyu.edu.

This article contains supporting information online at www.pnas.org/lookup/suppl/doi:10.1073/pnas.1017354108/-/DCSupplemental.

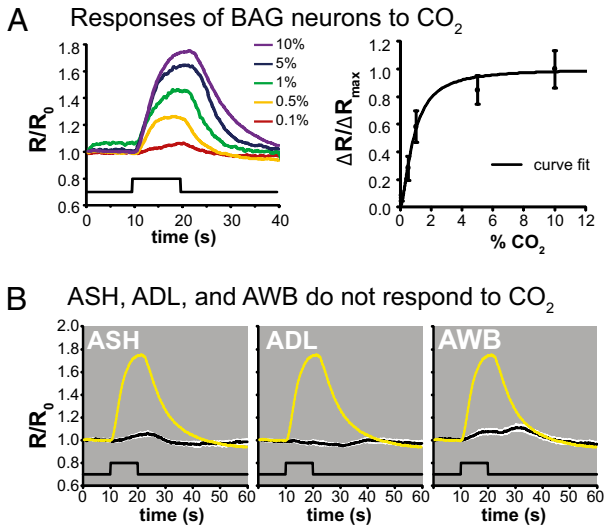

Fig. 1. BAG neurons are activated by CO_2. (*A Left*) BAG neuron cell bodies respond to CO_2. R/R_0 is the YFP to CFP ratio (R) divided by the average YFP to CFP ratio of the first 10 frames (R_0). (*A Right*) Dose-response curve for CO_2. $\Delta R/\Delta R_{max}$ is the maximal ratio change caused by presentation of a given CO_2 stimulus normalized to the maximal ratio change measured (evoked by 10% CO_2). (*B*) ASH, ADL, and AWB do not respond to 10% CO_2. The yellow trace is the average response of the BAG neurons to 10% CO_2. The white area around each trace represents the SEM; the lower black traces indicate the stimulus onset and duration (n = 5–18 animals for each condition or genotype). For all graphs, error bars represent SEMs.

exposure to 5% CO_2 (Fig. 2 *A* and *B*). Thus, *C. elegans* displays behavioral adaptation in response to prolonged CO_2 exposure.

To test whether behavioral adaptation to 5% or 10% CO_2 occurs at the level of the BAG neurons, we recorded the calcium response of BAG neurons evoked by prolonged exposure to CO_2. We found that a 1-min exposure to either 5% or 10% CO_2 caused an initial increase in BAG neuron calcium, which then dropped to below-baseline levels (Fig. 2 *C* and *D*). This drop in BAG neuron calcium was the result of desensitization; a 1-min exposure to 5% CO_2 blocked the calcium response to a subsequent 10% CO_2 stimulus (Fig. 2*E*). These results show that the BAG neurons desensitize during prolonged exposure to CO_2 and suggest that behavioral adaptation to CO_2 occurs at the level of the BAG sensory neuron.

cGMP-Gated Channel TAX-2/TAX-4 Is Required for BAG Neuron Responses to CO_2. CO_2 avoidance behavior by *C. elegans* requires multiple signaling pathways, including a cGMP, a G protein, an insulin, and a TGF-β pathway (13, 14). To test whether any of these pathways are required for the CO_2-evoked calcium response of the BAG neurons, we measured CO_2-evoked calcium transients of BAG neurons in animals that are mutant for these pathways and behaviorally defective in acute CO_2 avoidance. We found that mutations in *tax-2* and *tax-4*, which encode subunits of a cGMP-gated cation channel (29), eliminated the CO_2 calcium response of BAG neurons, indicating a direct requirement for TAX-2/TAX-4 in the signal transduction cascade that leads to CO_2 detection (Fig. 3).

We also found that G-protein signaling modulated BAG neuron responses to CO_2: mutation of *rgs-3*, which encodes a regulator of G protein signaling (30), resulted in reduced BAG neuron responses to CO_2 (Fig. 3). To test whether *rgs-3* functions in BAG neurons to regulate CO_2 responses, we expressed *rgs-3* specifically in the BAG neurons of *rgs-3* mutants and found that this expression restored normal CO_2 avoidance behavior (Fig. S5*A*). Because regulator of G protein signaling (RGS) proteins negatively regulate G-protein signaling (31), our results indicate that a G-protein signaling pathway negatively regulates BAG neurons.

A number of genes that are required for behavioral avoidance of CO_2 (13) were not required for CO_2-evoked calcium responses of the BAG neurons. These genes include *npr-1*, which

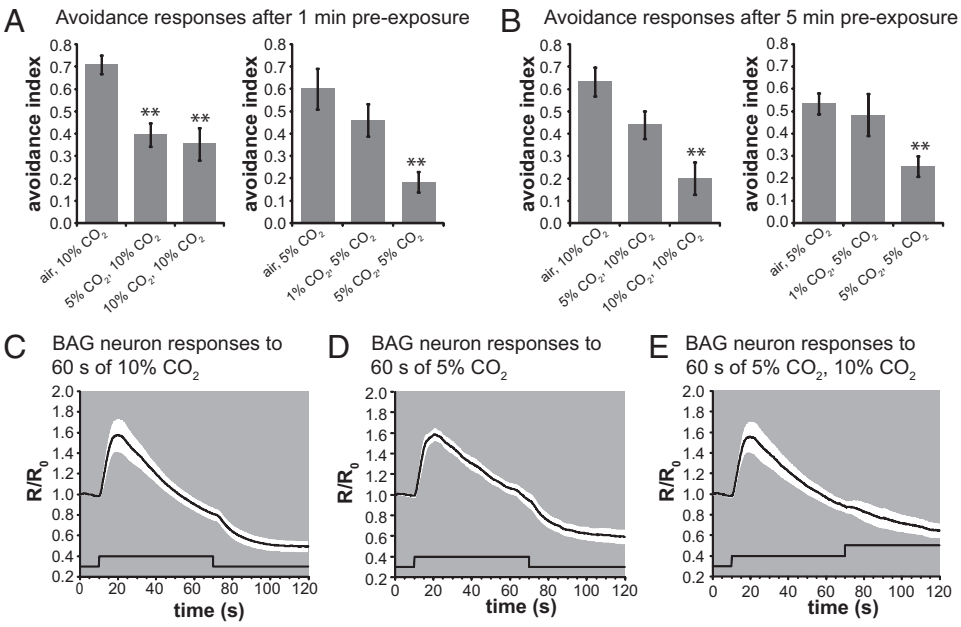

Fig. 2. Prolonged CO_2 exposure desensitizes BAG neurons. (*A* and *B*) Acute CO_2 avoidance after either a (*A*) 1-min or (*B*) 5-min exposure to CO_2. For each treatment condition, the stimulus used during the preexposure is indicated followed by the stimulus used for the acute avoidance assay (n = 11–15 trials for each treatment). (*C* and *D*) Prolonged pulses of either (*C*) 10% or (*D*) 5% CO_2 results in BAG neuron desensitization (n = 7 animals for each condition). (*E*) Prior exposure to 5% CO_2 blocks the response to 10% CO_2 (n = 7 animals). The white area around each trace represents the SEM; the lower black traces indicate the stimulus onset and duration.

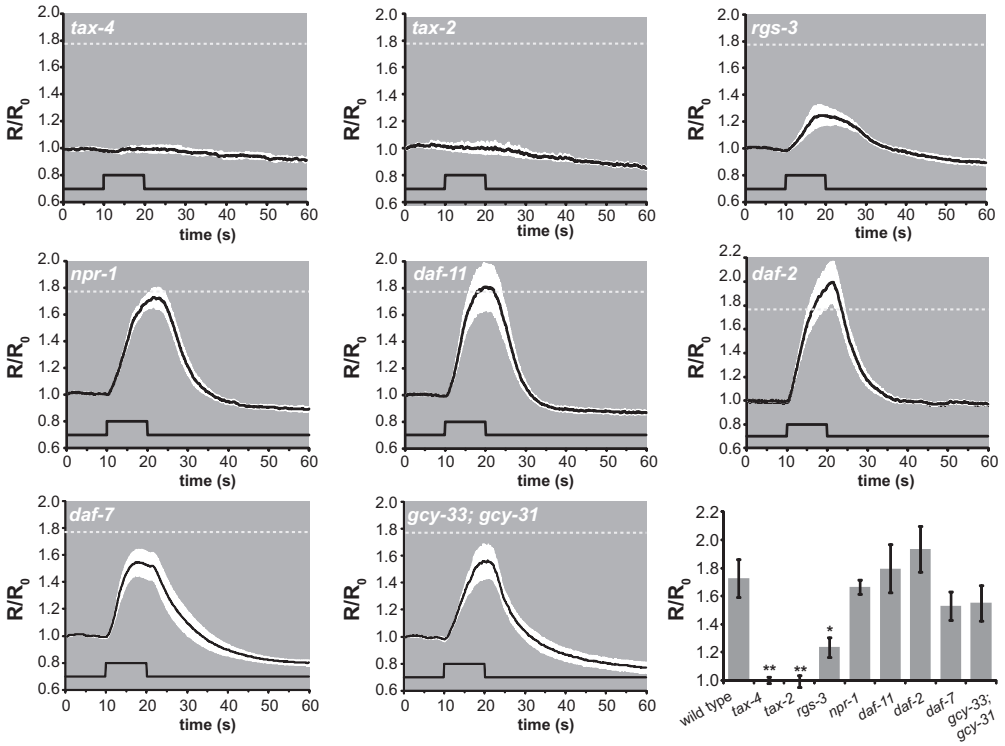

Fig. 3. A subset of genes required for acute CO_2 avoidance is required for activation of BAG neurons by CO_2. *tax-2* and *tax-4* mutations eliminate and an *rgs-3* mutation reduces CO_2-evoked calcium transients in the BAG neurons. *npr-1*, *daf-11*, *daf-2*, *daf-7*, and *gcy-33; gcy-31* mutations do not affect BAG neuron responses to CO_2 (n = 6–18 animals for each genotype). Dashed line indicates the mean maximum response of WT animals. The white area around each trace represents the SEM; the lower black traces indicate the stimulus onset and duration. (*Lower Right*) Summary of CO_2 responses for each genotype. Mean responses were calculated as the mean response after CO_2 exposure in the time interval 19.0–19.9 s, normalized to the mean response before CO_2 exposure in the time interval 0.4–1.3 s. Error bars represent average SEMs after CO_2 exposure (19.0–19.9 s).

encodes a G protein-coupled receptor similar to the neuropeptide Y receptor, *daf-11*, which encodes a receptor guanylate cyclase, *daf-2*, which encodes an insulin receptor, and *daf-7*, which encodes a TGF-β receptor. The BAG neurons of these mutants displayed robust calcium responses to CO_2, suggesting that these genes act either downstream of or in parallel to the calcium signal or that they act to regulate CO_2 avoidance in cells other than BAG neurons (Fig. 3). *daf-7* was reported to be expressed specifically in the amphid neurons ASI (32, 33), and expression of *daf-7* specifically in ASI neurons rescued the defect in CO_2 avoidance of *daf-7* mutants (Fig. S5*B*). Thus, *daf-7* acts in cells other than the BAG neurons to regulate acute CO_2 avoidance. Ablation of the ASI neurons does not affect CO_2 avoidance behavior (Fig. S5*C*), indicating that, unlike the BAG neurons, ASI neurons are not required for CO_2 detection. We also tested whether two BAG neuron-specific guanylate cyclases, *gcy-31* and *gcy-33*, are required for CO_2-evoked BAG neuron activity. *gcy-31* and *gcy-33* encode soluble guanylate cyclases that are required for BAG neuron responses to acute hypoxia (15). We found that the BAG neurons of *gcy-33; gcy-31* double mutants showed normal CO_2-evoked activity and that *gcy-33; gcy-31* mutants had normal behavioral responses to CO_2. Therefore, the CO_2- and O_2-sensing functions of the BAG neurons require distinct signaling pathways (Fig. 3 and Fig. S6).

Transcriptional Profiling of Embryonic BAG Neurons Identifies Signaling Molecules That Might Function in CO_2 Sensation. To identify signaling pathways that function in BAG neurons in CO_2 sensing, we performed transcriptional profiling of embryonic BAG neurons using Affymetrix *C. elegans* tiling arrays (Fig. S7). We identified 850 mRNA transcripts that were significantly enriched in the BAG neurons relative to the aggregate of all other embryonic cells (Dataset S1). The BAG neuron transcriptional profile is consistent with the role of BAG as a sensory neuron: the most highly enriched gene ontology terms include chemotaxis, response to external stimuli, response to chemical stimulus, and signaling [false discovery rate (FDR) ≤ 1%] (Fig. 4). BAG-enriched transcripts include a number of genes reported to be specifically expressed by BAG neurons (*gcy-31*, *gcy-33*, and *flp-17*) and genes with known roles in CO_2 sensing by BAG neurons (*tax-4* and *tax-2*) (13, 15, 34).

Among the genes most highly enriched in the BAG neurons is *gcy-9* (Fig. 4), which encodes a receptor-type guanylate cyclase (23). Nothing was previously known about the function of *gcy-9*, and reporter gene constructs for *gcy-9* resulted in either no expression or variable nonneuronal expression (23, 35). We found that *gcy-9* shows an approximately ninefold enrichment in BAG neurons relative to other embryonic cells, suggesting a role for *gcy-9* in BAG neuron function.

***gcy-9* Is Required for BAG Neurons to Respond to CO_2.** We examined the behavioral response of *gcy-9* mutants to CO_2 and found that *gcy-9* mutants did not respond to CO_2 (Fig. 5*A* and Fig. S8 *A* and *B*). To test whether *gcy-9* is required for CO_2-evoked activity of BAG neurons, we imaged the BAG neurons of *gcy-9* mutants. We found that the BAG neurons of *gcy-9* mutants did not show CO_2-evoked calcium transients, showing that *gcy-9* is necessary for BAG neuron responses to CO_2 (Fig. 5*B*). Expression of WT *gcy-9* specifically in the BAG neurons of *gcy-9* mutants rescued the defect in CO_2 avoidance behavior of *gcy-9* mutants and partially rescued the defect in CO_2-evoked neural activity of the BAG neuron (Fig. 5*C*), showing that *gcy-9* functions cell autonomously in CO_2 detection by the BAG neurons. Mutations in other guanylate cyclase genes did not affect acute CO_2 avoidance

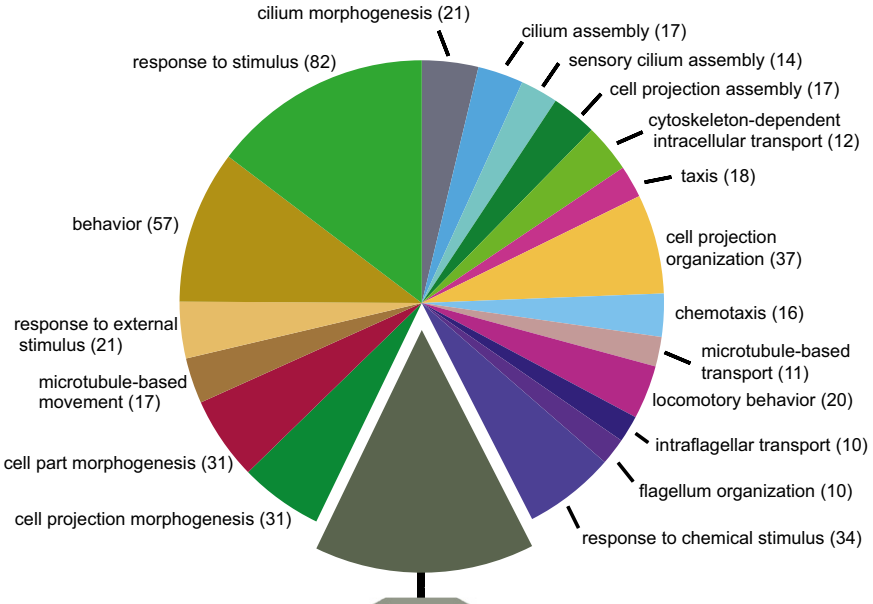

signaling (82)

Protein	Gene	FC
guanylate cyclase	*gcy-31*	9.4
guanylate cyclase	*gcy-9*	8.9
insulin-like peptide	*ins-1*	7.5
guanylate cyclase	*gcy-33*	7.0
arrestin domain	*Y49E10.24*	6.6
neuropeptide rec.	*F35G8.1*	5.0
synaptotagmin	*snt-1*	4.7
diacylglycerol kinase	*dgk-3*	4.6
ARF-like	*arl-13*	4.5
Ras-like	*F20D6.8*	4.1
IFT protein 80	*che-2*	3.9
EGF/Delta domain	*dsl-2*	3.9
calmodulin BP motif	*F39H12.3*	3.8
cGMP P-diesterase	*pde-1*	3.7
tyramine receptor	*tyra-3*	3.7

Fig. 4. Transcriptional profiling of embryonic BAG neurons. BAG neuron-enriched genes were organized according to gene ontology (GO) terms referring to biological process. The chart depicts the 15 most frequent GO terms, with the number of genes in each listed in parentheses. Shown below are the most abundant transcripts in the largest category (signaling), with fold change (FC) indicating relative enrichment in the BAG neuron profile.

(Fig. S8*C*) (13), with the exception of *daf-11*, which affects behavioral avoidance (13) but does not affect BAG neuron responses to CO_2 (Fig. 3). Thus, *gcy-9* is specifically required for CO_2-evoked BAG neuron activity. Taken together, our results suggest that GCY-9 acts upstream of TAX-2/TAX-4 in BAG neurons to mediate CO_2 detection.

Discussion

Our data indicate that the BAG neurons are activated by CO_2 and are likely the primary sensory neurons that detect CO_2. BAG neurons are sensitive detectors of CO_2, responding to CO_2 concentrations as little as twofold above the ambient level of ~0.04%. Behavioral adaptation to environmental CO_2 is also mediated by the BAG neurons, which desensitize during prolonged CO_2 stimuli.

The CO_2 avoidance circuit is modulated by input from other sensory neurons. Our data show that *daf-7* is required in ASI neurons for CO_2 avoidance behavior, suggesting that sensory cues detected by ASI regulate CO_2 avoidance. Because the BAG neurons of *daf-7* mutants respond normally to CO_2, it is possible that ASI acts on the neural circuit that mediates CO_2 avoidance downstream of the BAG neurons. This circuit remains to be defined. The primary synaptic output of the BAG neurons is onto five interneurons: the ventral cord interneurons AVA and AVE and the ring interneurons RIA, RIB, and RIG (21). In preliminary studies, we did not observe CO_2-evoked responses in the cell bodies of these interneurons. However, we cannot exclude the possibility that CO_2-evoked responses might be restricted to the processes of interneurons, which has been reported for interneurons in thermotaxis and chemotaxis circuits of *C. elegans* (36, 37).

It is also possible that the CO_2 avoidance circuit involves extrasynaptic signaling (for example, through neuropeptide secretion from BAG). Our analysis of BAG neuron transcripts identified more than a dozen neuropeptides that show enriched expression in the BAG neurons (Dataset S1). A role for neuropeptide signaling in the regulation of egg laying by the BAG neurons has been shown: the FMRF-amide like neuropeptide FLP-17 is secreted by the BAG neurons and acts on the G protein-coupled receptor EGL-6 on the HSN hermaphrodite-specific motor neurons to inhibit egg laying (34). FLP-17 peptides are not required for acute CO_2 avoidance (Fig. S9), indicating that BAG neurons regulate egg laying and avoidance behavior through distinct signaling pathways and circuits.

How do BAG neurons detect CO_2? CO_2 detection by insects requires the gustatory receptors GR21a and GR63a, which seem

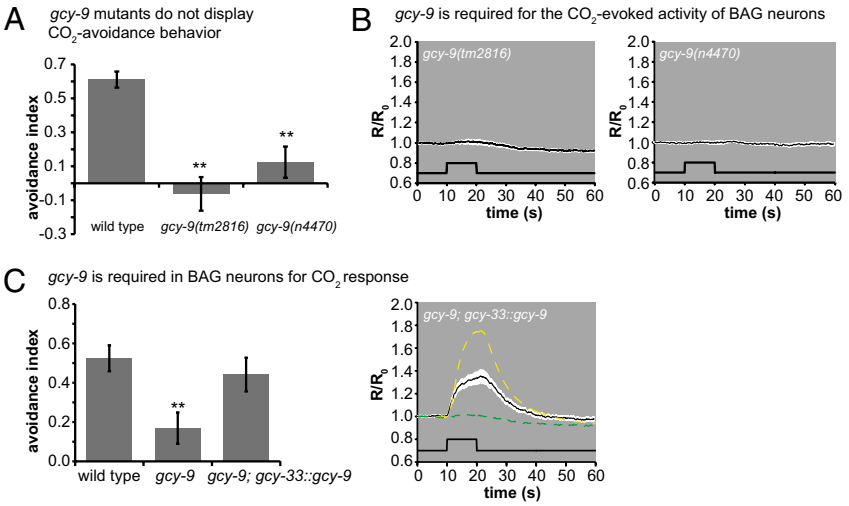

Fig. 5. *gcy-9* is required for CO_2 sensing by BAG neurons. (*A*) *gcy-9* mutants do not respond to CO_2 (n = 10–32 trials for each genotype). (*B*) *gcy-9* mutants do not show CO_2-evoked activity in the BAG neurons (n = 9 animals). (*C*) Expression of *gcy-9* specifically in the BAG neurons completely rescues CO_2 avoidance behavior (*Left*) and partially rescues CO_2-evoked calcium transients of BAG neurons (*Right*). *Left* has n = 22–39 trials for each genotype, and *Right* has n = 8 animals. The yellow dashed line shows the mean response of WT animals, and the green dashed line shows the mean response of *gcy-9(tm2816)* animals. The white area around each trace represents the SEM; the lower black traces indicated the stimulus onset and duration. For this experiment, CO_2 avoidance behavioral assays were performed on all three genotypes in parallel.

to act through a G-protein signaling pathway (16, 17, 38). By contrast, mammalian olfactory receptor neurons that respond to CO_2 express the receptor-type guanylate cyclase GC-D (8), which is activated by the CO_2 metabolite bicarbonate (20, 39). Because CO_2 sensing by the BAG neurons of *C. elegans* requires the receptor-type guanylate cyclase GCY-9, we propose that GCY-9 might function as a receptor for CO_2 or a metabolite of CO_2. GCY-9 is one of a large number of *C. elegans* guanylate cyclases (Fig. S10), many of which are expressed in small subsets of sensory neurons and are required for specific chemosensory behaviors (23, 29). Although some GCY proteins seem to function as chemoreceptors, others have been proposed to function downstream of G protein-coupled receptors (23, 40–42). It is, therefore, also possible that GCY-9 acts downstream of a yet to be identified receptor for CO_2.

GCY-9 orthologs are present in multiple nematode species, including the plant-parasitic nematodes *Heterodera glycines* and *Meloidogyne incognita* (43) and the human-parasitic nematode *Brugia malayi* (44). The requirement for GCY-9 in mediating a behavioral response to CO_2 and the importance of CO_2 as a host-seeking cue for many parasitic nematodes raise the possibility that compounds that block GCY-9 activity might be useful in the development of strategies for nematode control.

Materials and Methods

Standard techniques are listed in *SI Materials and Methods*.

Behavioral Assay for Acute CO_2 Avoidance. CO_2 assays were performed as previously described (13). Briefly, for each assay, about 10–20 L4 hermaphrodites were placed on 5-cm assay plates overnight and tested as young adults. Plates consisted of nematode growth medium (NGM) agar seeded with a thin lawn of *Escherichia coli* OP50 bacteria. Gases were medical grade certified mixes (Air Liquide) consisting of the indicated CO_2 concentration, 10% O_2, and the remaining percentage of N_2. A concentration of 10% CO_2 was used unless otherwise indicated. Two 50-mL syringes were filled with gas, one with CO_2 and one without CO_2. The mouths of the syringes were connected to tubes attached to Pasteur pipettes, and gases were pumped through the Pasteur pipettes using a syringe pump at a rate of 1.5 mL/min. Worms were exposed to gases by placing the tip of the Pasteur pipette near the head of a forward-moving worm, and a response was scored if the worm reversed within 4 s. An avoidance index was then calculated by subtracting the fraction of animals that reversed in response to the air control from the fraction of animals that reversed in response to the CO_2 (Fig. S2*A*).

Behavioral Assay for Adaptation to CO_2. For each assay, about five L4 hermaphrodites were placed on 9-cm assay plates overnight and tested as young adults. Plates consisted of NGM agar seeded with a thin lawn of OP50 in the center of the plate. Gas was pumped into the plate through a hole on one side of the lid at a rate of 1 L/min; a hole on the other side allowed gas to escape. Worms were preexposed to gas for either 1 or 5 min and then tested immediately in an acute avoidance assay.

Imaging BAG Neurons in Restrained Animals. Young adults were immobilized with cyanoacrylate veterinary glue (Surgi-Lock; Meridian Animal Health) on a cover glass coated with a 2% agarose pad made with 10 mM Hepes (pH 7.4). The cover glass was affixed to a custom-made air chamber. The specimen was illuminated with 435-nm excitation light and imaged using a 40× Nikon long-working distance objective (0.75 numerical aperture). The emission image was passed through a DV2 image splitter (Photometrics), and the CFP and YFP emission images were projected onto two halves of a cooled CCD camera (Andor). Images were acquired at 10 Hz, with exposure times between 10 and 50 ms. Gas perfusion was controlled by three-way valves (Numatics) driven by a custom-made valve controller unit. Excitation light, image acquisition, and hardware control were performed by the Live Acquisition software package (Till Photonics). Custom certified gas mixes used for imaging were obtained from Airgas.

Image Analysis. The mean pixel value of a background region of interest was subtracted from the mean pixel value of a region of interest that circumscribed the specimen. A correction factor, which we measured in images of samples that express only CFP, was applied to the YFP channel to compensate for bleed through of CFP emissions into the YFP channel ($YFP_{adjusted} = YFP - 0.86 \times CFP$). YFP to CFP ratios were normalized to the average value of the first 10 frames (1 s), and a boxcar filter of 5 frames (0.5 s) was applied to the time series.

Generating a Gene Expression Profile of Embryonic BAG Neurons. A synchronized population of *nIs242[gcy-33::GFP]* hermaphrodites was treated with hypochlorite to release embryos. Embryos were dissociated with chitinase as previously described (45, 46). GFP-labeled BAG neurons were isolated from the freshly dissociated suspension of embryonic cells by FACS; sorted cells were confirmed to be >80% BAG neurons by direct inspection in a fluorescent microscope. A reference population comprised of all viable embryonic cells was also collected by FACS. Dead cells were marked with propidium-iodide and excluded from these preparations. Sorting was performed with a Becton-Dickinson FACS-Aria (75-μm nozzle; ~15,000 events/s). Approximately 30,000 cells were obtained per sort. Cells were sorted directly into TRIzol LS for extraction with phenol chloroform. RNA was precipitated with isopropanol and purified using a ZYMO DNA-free RNA kit. RNA integrity and concentration were evaluated using an Agilent Bioanalyzer. RNA (1–2 ng) was amplified with the WT-Ovation Pico RNA Amplification System (NuGEN). Double-stranded (ds) cDNA was generated with a WT-Ovation Exon module (NuGEN), and it was fragmented and labeled with an Encore Biotin module (NuGEN) for application to the *C. elegans* Affymetrix 1.0R whole-genome tiling array; ds cDNA targets were used for hybridization, because all probes on the Affymetrix 1.0R array match a single DNA strand, whereas transcripts are derived from both strands. Tiling array results were obtained from three independent replicates (interse Pearson correlations ≥ 0.89). Methods for tiling array analysis are briefly summarized here. A more detailed de-

scription will be reported elsewhere. Unique PM (Perfect Match) probes from exonic regions of gene models were selected to generate a probe set for each gene listed in WormBase (WS199). Intensity values were quantile-normalized, and probe-specific effects were reduced by Robust Multichip Analysis (RMA) (47). An empirical null model of background expression was derived from intergenic probes, and genes with intensity values exceeding this threshold at ≤5% FDR were scored as significantly expressed genes (EGs). Transcripts that were significantly elevated in BAG neurons were identified by comparison with a reference dataset obtained from all viable embryonic cells. Differentially expressed genes were estimated using a linear model and Bayes-moderated *t* statistic (48, 49); 850 transcripts with FDR ≤ 10% and 1.5-fold elevated vs. the reference dataset were scored as significantly enriched in BAG neurons (Dataset S1). Gene ontology analysis was performed with the gene ontology (GO) enrichment analysis widget on the modENCODE intermine website (http://intermine.modencode.org). The 850 enriched BAG transcripts were uploaded to the modMINE website on July, 5, 2010; 464 transcripts were annotated with GO terms and compared with all genes for enrichment using the hypergeometric test with FDR ≤ 1%. All transcripts annotated with enriched GO terms are listed in Dataset S2.

Statistical Analysis. Statistical tests were performed using GraphPad Instat. Statistical comparisons were made using a one-way ANOVA with Dunnett's posttest, except that Fig. 1*A* used a paired *t* test and Fig. 5*A* used an unpaired *t* test. For Fig. 1*A*, the dose-response curve shows the least squares fit of a Hill equation to the data points, with a K_d of 0.9% CO_2 and a Hill coefficient of 1.6 (for all graphs, ***$P < 0.001$, **$P < 0.01$, and *$P < 0.05$). The GCY dendrogram was generated using ClustalW. The *gcy-9* intron–exon structure was generated using Exon–Intron Graphic Maker by Nikhil Bhatla (http://www.wormweb.org/exonintron).

ACKNOWLEDGMENTS. We thank Aravi Samuel, Chris Gabel, and Harrison Gabel (Harvard University, Cambridge, MA); Cori Bargmann (Rockefeller University, New York); Leon Avery (University of Texas Southwestern Medical Center, Dallas); Ikue Mori and Atsushi Kuhara (Nagoya University, Nagoya, Japan); Denise Ferkey (SUNY Buffalo, Buffalo, NY); Larry Salkoff (Washington University School of Medicine, St. Louis); Shohei Mitani (Tokyo Women's Medical University School of Medicine, Tokyo); Anne Hart (Brown University, Providence, RI); and the Caenorhabditis Genetics Center for strains and reagents. We thank the Vanderbilt Flow Cytometry Core and Vanderbilt Functional Genomics Shared Resource (VFGSR) for help with microarray experiments. We thank Julia Brandt and Sonya Aziz-Zaman for assistance in cloning the *gcy-9* cDNA. H.R.H. and P.W.S. are Investigators of the Howard Hughes Medical Institute. This work was supported by a Helen Hay Whitney postdoctoral fellowship (to E.A.H.), a National Institutes of Health Pathway to Independence award (to E.A.H.), National Institutes of Health Grants U01 HG004263 (to D.M.M.), R01 NS26115 (to D.M.M.), and R01 GM24663 (to H.R.H.), the Howard Hughes Medical Institute (P.W.S.), a Whitehead Fellowship for Junior Faculty in Biomedical and Biological Sciences (to N.R.), and funds from the Helen L. and Martin S. Kimmel Center for Biology and Medicine (to N.R.).

1. Haas W (2003) Parasitic worms: Strategies of host finding, recognition and invasion. *Zoology (Jena)* 106:349–364.
2. Guerenstein PG, Hildebrand JG (2008) Roles and effects of environmental carbon dioxide in insect life. *Annu Rev Entomol* 53:161–178.
3. Suh GS, et al. (2004) A single population of olfactory sensory neurons mediates an innate avoidance behaviour in *Drosophila*. *Nature* 431:854–859.
4. Faucher C, Forstreuter M, Hilker M, de Bruyne M (2006) Behavioral responses of *Drosophila* to biogenic levels of carbon dioxide depend on life-stage, sex and olfactory context. *J Exp Biol* 209:2739–2748.
5. Sharabi K, et al. (2009) Elevated CO_2 levels affect development, motility, and fertility and extend life span in *Caenorhabditis elegans*. *Proc Natl Acad Sci USA* 106:4024–4029.
6. Ziemann AE, et al. (2009) The amygdala is a chemosensor that detects carbon dioxide and acidosis to elicit fear behavior. *Cell* 139:1012–1021.
7. Lahiri S, Forster RE, 2nd (2003) CO_2/H(+) sensing: Peripheral and central chemoreception. *Int J Biochem Cell Biol* 35:1413–1435.
8. Hu J, et al. (2007) Detection of near-atmospheric concentrations of CO_2 by an olfactory subsystem in the mouse. *Science* 317:953–957.
9. Bensafi M, Frasnelli J, Reden J, Hummel T (2007) The neural representation of odor is modulated by the presence of a trigeminal stimulus during odor encoding. *Clin Neurophysiol* 118:696–701.
10. Bowen MF (1991) The sensory physiology of host-seeking behavior in mosquitoes. *Annu Rev Entomol* 36:139–158.
11. Haas W, et al. (2005) Behavioural strategies used by the hookworms *Necator americanus* and *Ancylostoma duodenale* to find, recognize and invade the human host. *Parasitol Res* 95:30–39.
12. Prot JC (1980) Migration of plant-parasitic nematodes towards plant roots. *Rev Nematol* 3:305–318.
13. Hallem EA, Sternberg PW (2008) Acute carbon dioxide avoidance in *Caenorhabditis elegans*. *Proc Natl Acad Sci USA* 105:8038–8043.
14. Bretscher AJ, Busch KE, de Bono M (2008) A carbon dioxide avoidance behavior is integrated with responses to ambient oxygen and food in *Caenorhabditis elegans*. *Proc Natl Acad Sci USA* 105:8044–8049.
15. Zimmer M, et al. (2009) Neurons detect increases and decreases in oxygen levels using distinct guanylate cyclases. *Neuron* 61:865–879.
16. Kwon JY, Dahanukar A, Weiss LA, Carlson JR (2007) The molecular basis of CO_2 reception in *Drosophila*. *Proc Natl Acad Sci USA* 104:3574–3578.
17. Jones WD, Cayirlioglu P, Kadow IG, Vosshall LB (2007) Two chemosensory receptors together mediate carbon dioxide detection in *Drosophila*. *Nature* 445:86–90.
18. Chen Y, et al. (2000) Soluble adenylyl cyclase as an evolutionarily conserved bicarbonate sensor. *Science* 289:625–628.
19. Luo M, Sun L, Hu J (2009) Neural detection of gases—carbon dioxide, oxygen—in vertebrates and invertebrates. *Curr Opin Neurobiol* 19:354–361.
20. Guo D, Zhang JJ, Huang XY (2009) Stimulation of guanylyl cyclase-D by bicarbonate. *Biochemistry* 48:4417–4422.
21. White JG, Southgate E, Thomson JN, Brenner S (1986) The structure of the nervous system of the nematode *Caenorhabditis elegans*. *Philos Trans R Soc Lond B Biol Sci* 314:1–340.
22. Nagai T, Yamada S, Tominaga T, Ichikawa M, Miyawaki A (2004) Expanded dynamic range of fluorescent indicators for $Ca^{(2+)}$ by circularly permuted yellow fluorescent proteins. *Proc Natl Acad Sci USA* 101:10554–10559.
23. Yu S, Avery L, Baude E, Garbers DL (1997) Guanylyl cyclase expression in specific sensory neurons: A new family of chemosensory receptors. *Proc Natl Acad Sci USA* 94:3384–3387.
24. Colbert HA, Smith TL, Bargmann CI (1997) OSM-9, a novel protein with structural similarity to channels, is required for olfaction, mechanosensation, and olfactory adaptation in *Caenorhabditis elegans*. *J Neurosci* 17:8259–8269.
25. Hilliard MA, et al. (2005) *In vivo* imaging of *C. elegans* ASH neurons: Cellular response and adaptation to chemical repellents. *EMBO J* 24:63–72.
26. L'Etoile ND, et al. (2002) The cyclic GMP-dependent protein kinase EGL-4 regulates olfactory adaptation in *C. elegans*. *Neuron* 36:1079–1089.
27. Chalasani SH, et al. (2010) Neuropeptide feedback modifies odor-evoked dynamics in *Caenorhabditis elegans* olfactory neurons. *Nat Neurosci* 13:615–621.
28. Hirotsu T, Iino Y (2005) Neural circuit-dependent odor adaptation in *C. elegans* is regulated by the Ras-MAPK pathway. *Genes Cells* 10:517–530.
29. Bargmann CI (2006) Chemosensation in *C. elegans*. *The C. elegans Research Community. WormBook*, Available at *www.WormBook.org*. Accessed December 7, 2010.
30. Ferkey DM, et al. (2007) *C. elegans* G protein regulator RGS-3 controls sensitivity to sensory stimuli. *Neuron* 53:39–52.
31. Ross EM, Wilkie TM (2000) GTPase-activating proteins for heterotrimeric G proteins: Regulators of G protein signaling (RGS) and RGS-like proteins. *Annu Rev Biochem* 69:795–827.
32. Ren P, et al. (1996) Control of *C. elegans* larval development by neuronal expression of a TGF-β homolog. *Science* 274:1389–1391.
33. Schackwitz WS, Inoue T, Thomas JH (1996) Chemosensory neurons function in parallel to mediate a pheromone response in *C. elegans*. *Neuron* 17:719–728.
34. Ringstad N, Horvitz HR (2008) FMRFamide neuropeptides and acetylcholine synergistically inhibit egg-laying by *C. elegans*. *Nat Neurosci* 11:1168–1176.
35. Ortiz CO, et al. (2006) Searching for neuronal left/right asymmetry: Genomewide analysis of nematode receptor-type guanylyl cyclases. *Genetics* 173:131–149.
36. Clark DA, Biron D, Sengupta P, Samuel AD (2006) The AFD sensory neurons encode multiple functions underlying thermotactic behavior in *Caenorhabditis elegans*. *J Neurosci* 26:7444–7451.
37. Chalasani SH, et al. (2007) Dissecting a circuit for olfactory behaviour in *Caenorhabditis elegans*. *Nature* 450:63–70.
38. Yao CA, Carlson JR (2010) Role of G-proteins in odor-sensing and CO_2-sensing neurons in *Drosophila*. *J Neurosci* 30:4562–4572.
39. Sun L, et al. (2009) Guanylyl cyclase-D in the olfactory CO_2 neurons is activated by bicarbonate. *Proc Natl Acad Sci USA* 106:2041–2046.
40. Ortiz CO, et al. (2009) Lateralized gustatory behavior of *C. elegans* is controlled by specific receptor-type guanylyl cyclases. *Curr Biol* 19:996–1004.
41. Gray JM, et al. (2004) Oxygen sensation and social feeding mediated by a *C. elegans* guanylate cyclase homologue. *Nature* 430:317–322.
42. Kim K, et al. (2009) Two chemoreceptors mediate developmental effects of dauer pheromone in *C. elegans*. *Science* 326:994–998.
43. Fitzpatrick DA, O'Halloran DM, Burnell AM (2006) Multiple lineage specific expansions within the guanylyl cyclase gene family. *BMC Evol Biol*, 10.1186/1471-2148-6-26.
44. Ghedin E, et al. (2007) Draft genome of the filarial nematode parasite *Brugia malayi*. *Science* 317:1756–1760.
45. Christensen M, et al. (2002) A primary culture system for functional analysis of *C. elegans* neurons and muscle cells. *Neuron* 33:503–514.
46. Fox RM, et al. A gene expression fingerprint of *C. elegans* embryonic motor neurons. *BMC Genomics*, 10.1186/1471-2164-6-42.
47. Irizarry RA, et al. (2003) Exploration, normalization, and summaries of high density oligonucleotide array probe level data. *Biostatistics* 4:249–264.
48. Smyth GK (2004) Linear models and empirical Bayes methods for assessing differential expression in microarray experiments. *Stat Appl Genet Mol Biol*, 10.2202/1544-6115.1027.
49. Smyth GK (2005) Limma: Linear models for microarray data. *Bioinformatics and Computational Biology Solutions Using R and Bioconductor*, eds Gentleman R, Carey VJ, Huber W, Irizarry RA, Dudoit S (Springer, New York), pp 397–420.